

***Institution's repository*** (“Petru Poni” Institute of Macromolecular  
Chemistry, Iasi, Romania)

*Green Open Access:*

Authors' Self-archive manuscript

(enabled to public access in ***October 2019***, after 24-month embargo period)

*This manuscript was published as formal in:*

**European Polymer Journal 2017, 95, 127-137**

**DOI:** 10.1016/j.eurpolymj.2017.08.006

<https://doi.org/10.1016/j.eurpolymj.2017.08.006>

***Title:***

**Poly(azomethine-phenothiazine)s with efficient emission in solid state**

Luminita Marin<sup>1\*</sup>, Andrei Bejan<sup>1</sup>, Daniela Ailincăi<sup>1</sup>, Dalila Belei<sup>2</sup>

<sup>1</sup> "Petru Poni" Institute of Macromolecular Chemistry of Romanian Academy, Iasi, Romania

<sup>2</sup> "Alexandru Ioan Cuza" University, Department of Organic Chemistry, Iasi, Romania

\*email: lmarin@icmpp.ro

## **Abstract**

A series of poly(azomethine-phenothiazine)s was synthesized by using the reaction of 10-methyl-phenothiazine-3,7-dicarbaldehyde with diamines containing fluorene chromophore or polyethylene glycol (PEG) flexible spacer. The polymers were structurally characterized by <sup>1</sup>H-NMR and FTIR spectral techniques, elemental analysis and wide-angle X-ray diffraction. Their thermal properties were monitored by using variable temperature polarized light microscopy whilst their photophysical behaviour was demonstrated by using UV-vis absorption and photoluminescence spectroscopy. All of these polymers were found to emit green light with high quantum yield, in both solution and solid state. The emission efficiency in solid state was further improved by mixing the fluorene containing polymers with the PEG containing one, when continuous films with quantum efficiency of up to 16 % were obtained.

**Keywords:** polyazomethine, phenothiazine, luminescence, high quantum yield

## **1. Introduction**

Azomethine linkage, also known as imine or Schiff base is a covalent dynamic connection used in building up polymeric and supramolecular architectures with various functionalities, from simple thermostable materials [1] to more complex structures such as coordination compounds and liquid crystals [2-6] or adaptive materials capable to respond under the environment pressure such as self-healing films [7, 8], membranes [9], and hydrogels [10-12], artificial water

channels [13], DNA vectors [14], and so on. The same simple azomethine connection has been demonstrated to yield stable systems with potential applications for optoelectronics [15-20] as well as dynamic systems with adaptive properties [7-14], its features depending mainly on the connecting building blocks. The good stability of the azomethine compounds is related to the donor-acceptor character of the building blocks which promotes the electron conjugation, resulting in the shift of the reaction equilibrium towards the imine products. Compared to their vinyl isoelectronic counterparts, the use of the azomethine bridge to design functional materials of optoelectronic devices brings in the advantage of easy preparation in mild reaction conditions and easy purification [21]. By connecting donor – acceptor heterocyclic units, the azomethine bridge is constrained to adopt a coplanar geometry with good electronic conjugation with promising performances in various organic electronics. For example, low molecular weight azomethines with values of conductance comparable to the ones reported for vinyl-based analogues [21]; azomethines based on triphenylamine donors with good film-forming ability as well as high power conversion efficiency of 6.68 in perovskite solar cells [22]; thiopheno-azomethines with good charge carrier mobility of  $3 \times 10^{-5} \text{ cm}^2/\text{Vs}$  in field effect transistor configurations comparable to that of analogue thiophene vinylene compounds [23]. It was demonstrated that the introduction of the imine linkage results in an enhancement the electroluminescence efficiency as well as carrier transport properties of indenofluorene derivatives, due to its electron-withdrawing ability which increases the conjugation with indeno donor [24]. Moreover, the azomethines have the advantage of possessing doping ability which can tune their processability, ordering degree, light emission and conductivity [25]. Their ability to form thermotropic mesophases or molecular glasses can be used in the processing films of good quality with tuned morphology and thus improved properties [26-29]. This short literature survey led to the conclusion that polyazomethines with excellent optoelectronic properties can be obtained by combining the electron withdrawing imine linkage with different

donor moieties. Our previous studies on some azomethine dimers revealed that the phenothiazine heterocycle is of particular interest for obtaining materials with optoelectronic applications. It was also established that its bent structure promotes higher intermolecular distances which facilitate high luminescence efficiency, comparable to that of the prototypical polyfluorene [29].

In this context, the current paper reports the synthesis and characterization of a series of donor-acceptor (D-A) poly(azomethine-phenothiazine)s as potential materials for optoelectronic applications. Their thermotropic and photo-physical properties were studied in detail and a method of improving their quantum efficiency in solid state has been proposed.

## **2. Experimental**

### **2.1 Materials**

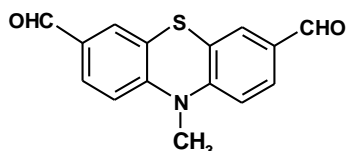
*3.1.1. 2,7-diaminofluorene 97%, 9,9-bis(p-aminophenyl)-fluorene 98% and poly(ethylene glycol)bis(3-aminopropyl) terminated (PEG,  $M_n \sim 1500 \text{ g mol}^{-1}$ ) were purchased from Aldrich and used as supplied. 10-methyl-10H-phenothiazine-3,7-dicarbaldehyde has been synthesized in our laboratory adapting a published procedure [30]. The solvents were dried on molecular sieves before their use.*

### **2.2 Synthesis**

#### ***10-methyl-10H-phenothiazine-3,7-dicarbaldehyde***

The Vilsmeier reagent was prepared by adding dropwise 30 mL of phosphoryl chloride (0.28 mol) to a mixture of DMF (40 mL, 0.56 mol) and 1,2-dichloroethane (30 mL), at 0 °C. Then, 10-methyl-10H-phenothiazine (3 g, 0.014 mol) was added to the Vilsmeier reagent under vigorous stirring, slowly heated up to 90 °C, and maintained for 2 days. The reaction mixture was then poured into distilled water (200 mL), and the pH was adjusted to 8.0 with a solution of sodium acetate. The organic phase was extracted with ethyl acetate, dried over anhydrous

magnesium sulphate and concentrated by rotary evaporation. The crude product was further purified by column chromatography on silica-gel using ethyl acetate/cyclohexane (1/5, v/v) as eluent. The pure product was obtained as a yellow powder with a total yield of 15%. Melting point: 178-180 °C.

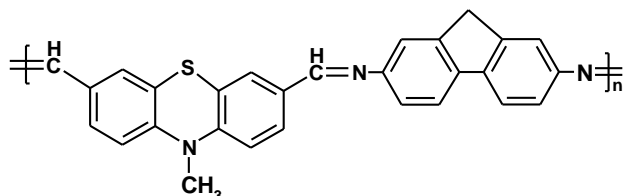


**FTIR:** 2953, 2865 (C-H stretch of the CH<sub>3</sub> unit of phenothiazine ring), 1675 (-CH=O stretch), 1576, 1547, 1468, (C=C stretch of aromatic rings), 811 (C-H bend of aromatic units). **<sup>1</sup>H NMR (400.13 MHz, DMSO-d<sub>6</sub>, ppm):** 3,47 (s, 3H, CH<sub>3</sub>), 7,2 (d, J = 8,4 Hz, 2H, 2 x CH<sub>ar</sub>), 7,66 (s, 2H, 2 x CH<sub>ar</sub>), 7,78 (d, J = 8,4 Hz, 2H, CH<sub>ar</sub>), 9,84 (s, 2H, -CHO). Elemental analysis calc. for the repeating unit C<sub>15</sub>H<sub>11</sub>NO<sub>2</sub>S (269): C 66.9; H 4.12; N 5.2; S 11.9. Found: C 70.23; H 4.34; N 5.41; S 12.01.

The synthetic pathway for obtaining the polyazomethines reported in this study includes the condensation reaction between 10-methyl-phenothiazine-3,7-dicarbaldehyde and three different diamines: 2,7-diaminofluorene, 9,9-bis(p-aminophenyl)-fluorene, and poly(ethylene glycol) diamine (Mw=2000). An equimolar mixture of dialdehyde/diamine was used to give the alternant polymers **PF**, **PFR**, **PPEG**. A mixture of dialdehyde and the two fluorene containing diamines in the molar ratio of 1/0.5/0.5 was used to obtain the random copolymer **PFRF**. A typical polycondensation procedure (**PF**) is following presented: 0.134 g (0.5 mmol) of 10-methyl-phenothiazine-3,7-dicarbaldehyde and 0.098g (0.5 mmol) of 2,7-diaminofluorene were charged into a bottom round flask and dissolved in 4.6 mL THF to give a 5% solution. The reaction mixture was gently refluxed overnight under vigorously magnetically stirring, until a yellow powder precipitated out of solution. The reaction mixture was poured into methanol and filtered. The crude polymer was further purified by refluxing for two hours in dry methanol, followed by hot filtration to remove the unreacted monomers. In the

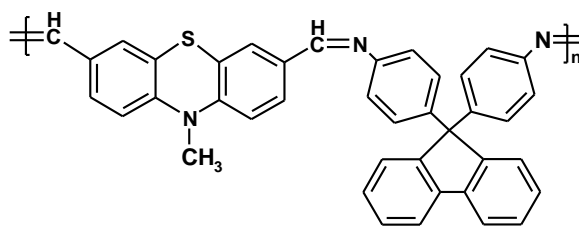
case of the polymer containing PEG units, because of its high solubility, the reaction mixture was concentrated by rotary evaporation and used as such further. The structure of the polymers was confirmed by elemental analysis, FTIR and NMR spectroscopy, as follows.

**PF**, orange powder, 73% yield,  $M_n$  7 300,  $M_w$  8100



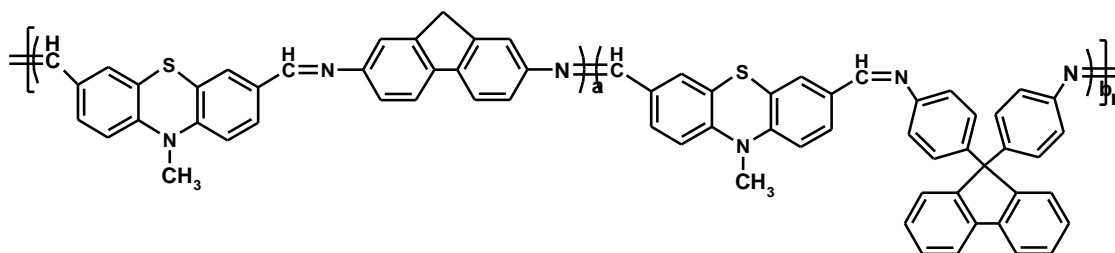
**FTIR (ATR,  $\text{cm}^{-1}$ ):** 3056 (=C-H stretch of the aromatic rings), 2960-2882 (C-H stretch of the aliphatic units ( $\text{CH}_3$  unit of phenothiazine ring and  $\text{CH}_2$  unit in fluorene)), 1683 (-CH=O stretch), 1620 (-CH=N- stretch), 1582, 1500 (C=C stretch of aromatic rings), 813 (C-H bend of aromatic units).  **$^1\text{H NMR}$  (400.13 MHz, DMSO- $d_6$ , ppm)**  $\delta$  = 9.85 (s,  $\text{CH}=\text{O}$ ), 8.7 (s,  $\text{CH}=\text{N}$ ), 7.80-6.52 (aromatic protons), 4.27 (s,  $\text{CH}_3$ ), 3.52 (s,  $\text{CH}_2$ ). Elemental analysis calc. for the repeating unit  $\text{C}_{28}\text{H}_{19}\text{N}_3\text{S}$  (429): C 78.29; H 4.46; N 9.78; S 7.46. Found: C 77.67; H 4.61; N 9.92; S 7.38.

**PFR**, deep yellow powder, 95% yield,  $M_n$  8 000,  $M_w$  8 900



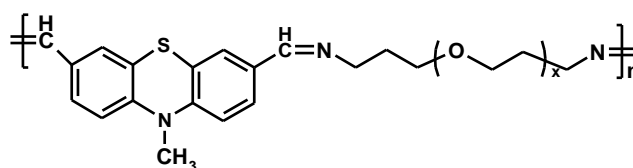
**FTIR (ATR,  $\text{cm}^{-1}$ ):** 3056-3023 (=C-H stretch of the aromatic rings), 2971-2869 (C-H stretch of the aliphatic  $\text{CH}_3$  units), 1688 (-CH=O stretch), 1621 (-CH=N- stretch), 1577, 1508 (C=C stretch of aromatic rings), 816-737 (C-H bend of aromatic units).  **$^1\text{H NMR}$  (400.13 MHz, DMSO- $d_6$ , ppm)**  $\delta$  = 9.83 (s,  $\text{CH}=\text{O}$ ), 8.47 (s,  $\text{CH}=\text{N}$ ), 7.56-6.39 (aromatic protons), 4.27 (s,  $\text{CH}_3$ ). Elemental analysis calc. for the repeating unit  $\text{C}_{40}\text{H}_{27}\text{N}_3\text{S}$  (581): C 82.02; H 5.33; N 7.17; S 5.47. Found: C 81.52; H 5.47; N 7.23; S 5.58.

**PFRF**, deep yellow powder, 87% yield,  $M_n$  8 600,  $M_w$  9 800



**FTIR (ATR,  $\text{cm}^{-1}$ ):** 3053-3027 ( $=\text{C}-\text{H}$  stretch of the aromatic rings), 2949-2818 ( $\text{C}-\text{H}$  stretch of the aliphatic units), 1686 ( $-\text{CH}=\text{O}$  stretch), 1621 ( $-\text{CH}=\text{N}-$  stretch), 1582, 1504 ( $\text{C}=\text{C}$  stretch of aromatic rings), 816-733 ( $\text{C}-\text{H}$  bend of aromatic units).  **$^1\text{H NMR}$  (400.13 MHz,  $\text{DMSO}-d_6$ , ppm)**  $\delta$  = 9.83 (s,  $\text{CH}=\text{O}$ ), 8.23 (s,  $\text{CH}=\text{N}$ ), 7.98-6.39 (aromatic protons), 4.27 (s,  $\text{CH}_3$ ), 3.52 (s,  $\text{CH}_2$ ). Elemental analysis calc. for the repeating unit  $\text{C}_{68}\text{H}_{46}\text{N}_6\text{S}_2$  (1011): C 80.76; H 4.59; N 8.31; S 6.34. Found: C 81.13; H 5.21; N 8.76; S 6.59.

**PPEG**, yellow solid, 97% yield,  $M_n$  13 400,  $M_w$  15 300



**FTIR (ATR,  $\text{cm}^{-1}$ ):** 2947 ( $=\text{C}-\text{H}$  stretch of the aromatic rings), 2883-2742 ( $\text{C}-\text{H}$  stretch of the aliphatic units), 1679 ( $-\text{CH}=\text{O}$  stretch), 1638 ( $-\text{CH}=\text{N}-$  stretch), 1579-1465 ( $\text{C}=\text{C}$  stretch of aromatic rings), 1100 ( $\text{C}-\text{O}-\text{C}$  stretch), 959-840 ( $\text{C}-\text{H}$  bend of aromatic units).  **$^1\text{H NMR}$  (400.13 MHz,  $\text{DMSO}-d_6$ , ppm)**  $\delta$  = 9.83 (s,  $\text{CH}=\text{O}$ ), 8.22 (s,  $\text{CH}=\text{N}$ ), 7.99-6.83 (aromatic protons), 4.27 (s,  $\text{CH}_3$ ), 3.5 (superposed to the  $\text{DMSO}-\text{H}_2\text{O}$ ,  $\text{CH}_2-\text{O}$ ), 2.3(m,  $=\text{N}-\text{CH}_2$ ), 1.7(m,  $\text{CH}_2-\text{CH}_2-\text{CH}_2$ ). Elemental analysis calc. for the repeating unit  $\text{C}_{84}\text{H}_{149}\text{O}_{32}\text{N}_3\text{S}$  (1737): C 58.03; H 8.57; N 2.4; S 1.8. Found: C 58.49.13; H 8.91; O 30.02 N 2.75; S 2.09.

### 2.3 Methods

Determination of carbon, hydrogen, nitrogen and sulphur content of the compounds has been performed on a 2400 Series II CHNS Perkin Elmer elemental analyser.

Infrared (IR) spectra were recorded on a FTIR Bruker Vertex 70 Spectrophotometer, by ATR technique, on powders and thin films. Similar spectra were obtained.

The liquid state  $^1\text{H-NMR}$  spectra were recorded on a BRUKER Avance DRX 400 MHz spectrometer, equipped with a 5 mm direct detection QNP probe with z-gradients. The spectra were recorded at room temperature, in DMSO-d<sub>6</sub>. The chemical shifts are reported as  $\delta$  values (ppm) relative to the residual peak of the solvent.

Molecular weight distributions of the polymers were measured by gel permeation chromatography (GPC) analysis carried out on a PL-EMD 950 Evaporative Light Scattering Detector instrument, using DMF as eluent and standard polystyrene samples for calibration. The measurements were carried out at 60 °C.

UV–Vis absorption and photoluminescence spectra were recorded on a Carl Zeiss Jena SPECORD M42 and a Perkin Elmer LS 55 spectrophotometer, respectively, in diluted DMF solutions of  $10^{-5}$  M concentration, using 10 mm quartz cells, at room temperature. The fluorescence quantum yield ( $\Phi$ ) of the samples, in solution and film, was measured on a FluoroMax-4 spectrofluorometer equipped with a Quanta-phi integrating sphere accessory Horiba Jobin Yvon, by exciting at the maximum absorption, at room temperature. The concentration of the solution was optimized to obtain an absorbance around 0.055. The slit widths and detector parameters were optimized to maximize but not saturate the excitation Rayleigh peak, in order to obtain a good optical luminescence signal-to-noise ratio.

The thermotropic behaviour of the polymers was studied by observing the textures with an Olympus BH-2 polarized light microscope equipped with a THMS 600 hot stage and LINKAM TP92 temperature control system.

Wide Angle X-ray Diffraction (WAXD) was performed on a Bruker D8 Avance diffractometer, using the Ni-filtered Cu K $\alpha$  radiation ( $\lambda = 0.1541$  nm). The working conditions



were 36 kV and 30 mA. All diffractograms were registered on powder samples, in the 2-40° range, at room temperature, and reported as observed.

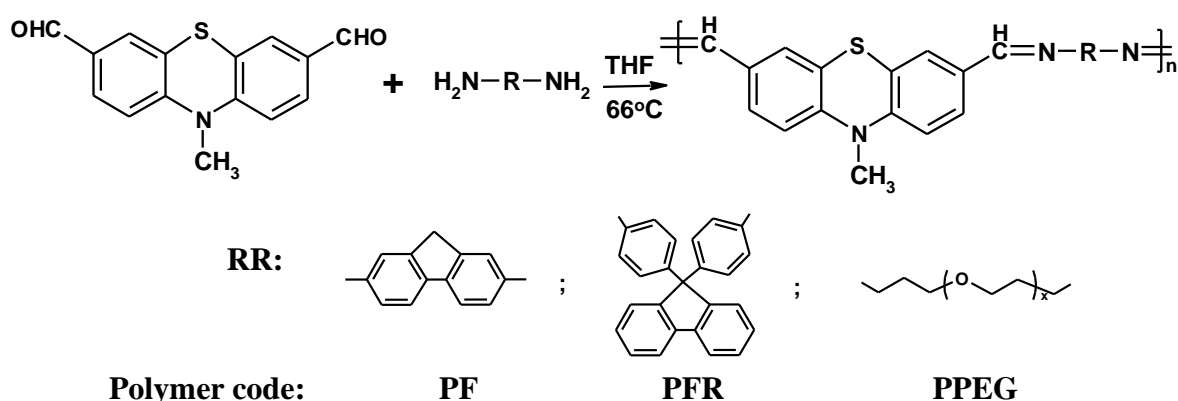
The solubility tests were performed by dissolving 1 mg sample in 10 mL solvent (dimethylsulfoxide, dimethylformamide, chloroform, acetonitrile, acetone and water).

Thin films of polymers were obtained by successive castings of DMF solutions ( $10^{-5}$  M) on quartz supports heated at 60 °C. They were kept 12 hours on the heated plates, and then dried in a vacuum oven, at 60 °C, for 24 hours.

### 3. Results and discussions

#### 3.1 Synthesis and structural confirmation

A series of four acceptor-donor polyazomethines was synthesized by the condensation reaction of a dialdehyde based on phenothiazine donor with diamines based on fluorene acceptor (**PF**, **PFR**) or poly(ethylene glycol) flexible unit (**PPEG**) (Scheme 1) to give alternant polymers. The fluorene moiety of the diamines was connected in the main chain (**PF**) or as a bulky unit (**PFR**). In order to combine their complementary properties, a 1:1 mixture of the two types of fluorene diamines was used to give a random polyazomethine (**PFRF**). The polymers structure and their codes are presented in the experimental section.



**Scheme 1.** Synthesis of phenothiazine based polyazomethines

The formation of the imine bridge has been confirmed by FTIR spectroscopy, based on appearance of the characteristic stretching vibration in the range of  $1620\text{ cm}^{-1}$  –  $1638\text{ cm}^{-1}$ , as

well as the presence of the other characteristic absorption bands (see experimental part) [31-33]. The imine band was shifted to higher wavenumbers for PEG based polymer, due to the lower conjugation of the imine bond connecting an aromatic unit with an aliphatic one [34]. The bands originating from the vibration of the aldehyde ( $1686\text{ cm}^{-1}$ ) and the amine units ( $3500\text{ cm}^{-1}$  region) can be observed on the FTIR as they are end groups. The imine formation during the polycondensation reaction was also confirmed by the  $^1\text{H}$ -NMR spectra, based on the occurrence of the characteristic chemical shift between 8.2 and 8.7 ppm (see experimental part). Representative FTIR and  $^1\text{H}$ -NMR spectra were given in Figure 1.

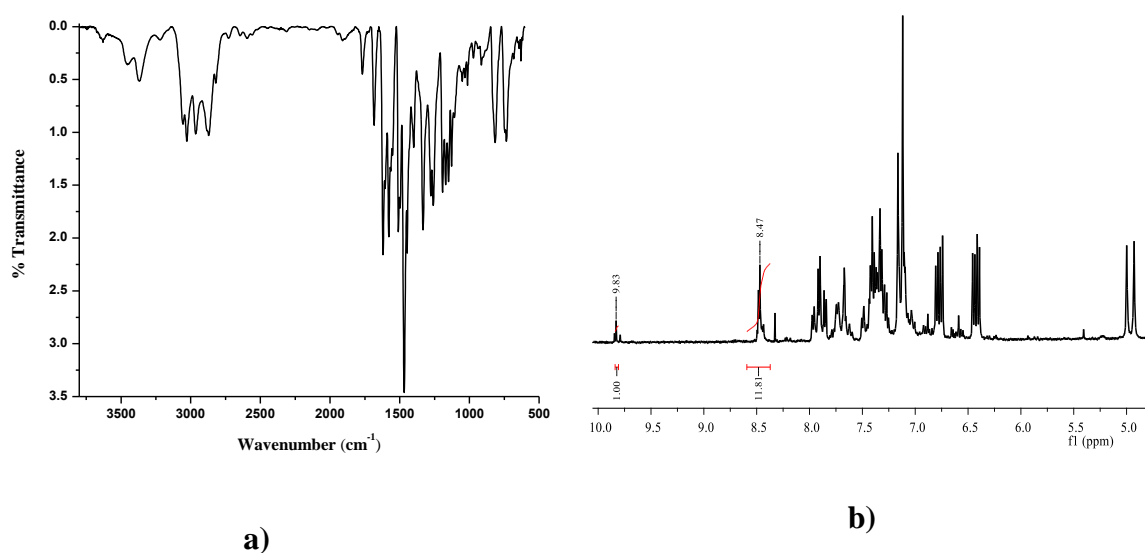


**Figure 1.** FTIR (a) and  $^1\text{H}$ -NMR (b) spectra of **PFR**

The polymer containing PEG units (**PPEG**) was completely soluble in all the tested solvents. The polymers containing bulky fluorene group (**PFR**, **PFRF**) were completely soluble in DMSO and DMF, insoluble in water and partially soluble in the other solvents, whilst the polymer containing fluorene unit in the main chain (**PF**) was partial soluble in DMSO and DMF only.

The polymeric nature of the studied polymers was investigated by gel permeation chromatography in DMF solutions, at  $60\text{ }^\circ\text{C}$ . The molecular weight values  $M_w$  ranged from 8

000 to 15 000, the  $M_n$  from 7 000 to 13 000 and the polydispersity index  $M_w/M_n$  from 1.14 to 1.22 (see experimental part). Considering the molecular weight of the repeating unit in the polymers, a polycondensation degree of approximately 15 could be estimated for the polymers containing fluorene units, and 150 for the polymer containing PEG, values which indicate fairly good molecular weights for this class of polymers [1].

### **3.2 X-ray diffraction**

The X-ray diffraction of the studied polymers exhibited different profiles, in terms of shape and intensity of the reflection bands, in accordance with their structure (Figure 2).

Therefore, the **PPEG** poly(azomethine-phenothiazine) showed a similar XRD pattern with the polyethylenglycol, indicating its dominance during the crystallization process. The two sharp, intense reflection peaks correspond to the interplanar crystal spacing of a monoclinic system [35].

The **PF** polymer showed an X-ray diffractogram with quite sharp reflection peaks in both, low and wide angle domains – signature of a highly ordered architecture, due to its rigid backbone which facilitated the self-ordering from solution. In contrast, the **PFR** polymer showed a broad reflection band with two maxima around 11 and 20 °, indicating a semicrystalline state with low degree of ordering, because of the pendant bulky fluorene units which hindered the intermolecular forces between the backbones. The diffractogram of the **PFRF** polymer appeared to be a combination of the **PF** and **PFR** diffractograms: a broad band with sharper reflections above it, located in similar positions as in **PF** but of lower intensity. The **PFRF** diffractogram reflects the ability of self-ordering of the rigid segments, hindered by the pendant fluorene moieties randomly distributed on the polymer backbone.

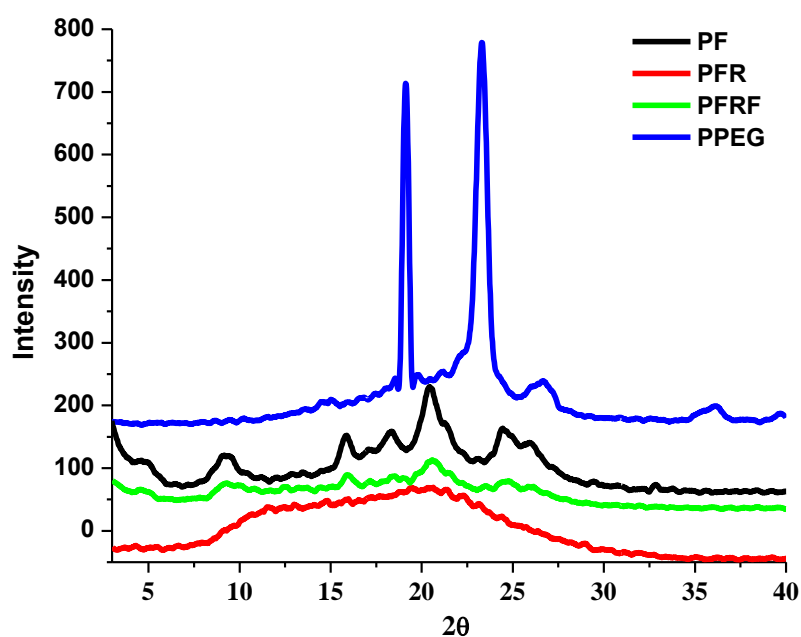


**Figure 2.** Wide angle X-ray diffraction of the poly(azomethine-phenothiazine)s

### 3.3 Thermotropic behaviour

The thermal properties of the samples were monitored by polarized light microscopy in a heating-cooling-heating scan, from room temperature up to 360 °C. All polyazomethines exhibited birefringence at room temperature, in accordance to their semicrystalline nature (Figure 3a,b). During the first heating scan up to 360 °C, the polyazomethines containing fluorene units in the main chain (**PF**, **PFRF**) didn't show a melting transition, but only a slight colour change, indicating the occurring of decomposition. The alternant polyazomethine containing fluorene unit as a bulky group (**PFR**) exhibited a slight softening around 260 °C, but the polymer didn't melt when heated up to 360 °C. The polymer containing PEG flexible units (**PPEG**) completely melted during the first heating scan, at 49 °C, and it froze into an amorphous glass during the cooling scan. The amorphous glass further slowly crystallized during 24 hours in spherulites with four symmetrically disposed sectors forming the Maltese Cross (Figure 3c).

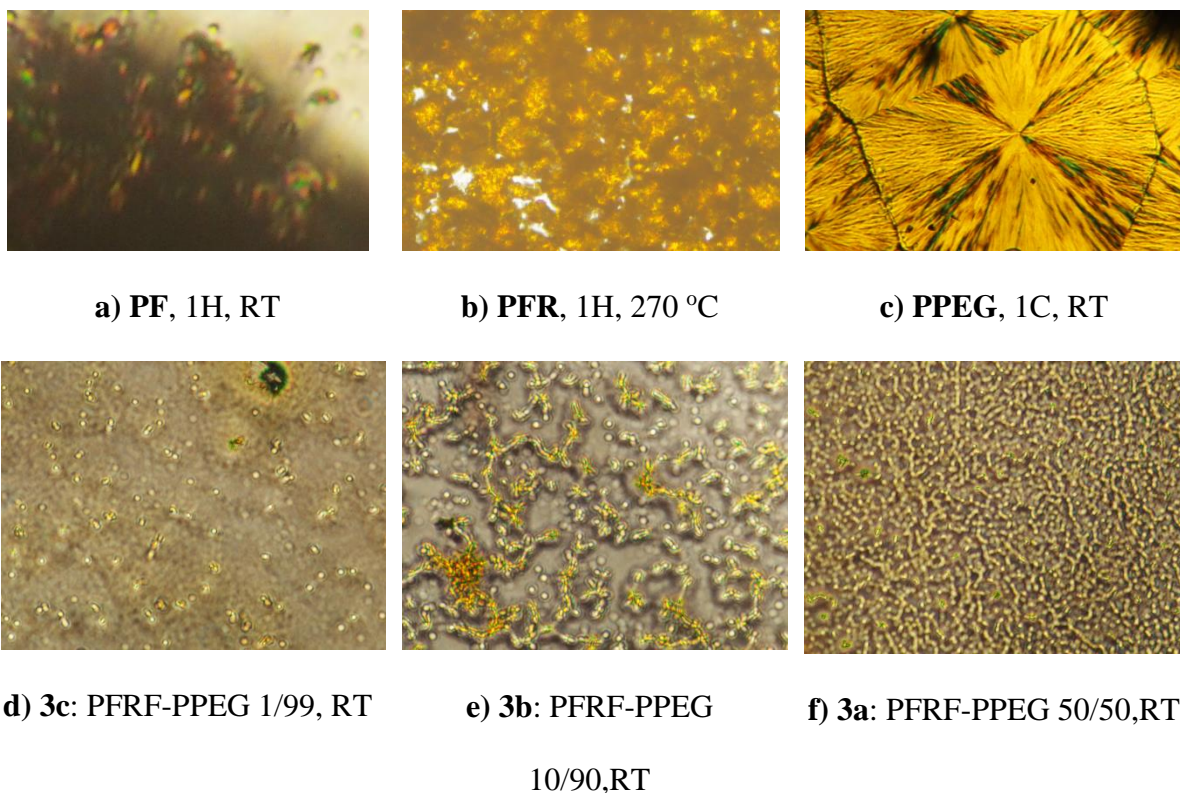


**Figure 3.** Representative POM images of the studied polyazomethines and their mixtures (RT: room temperature; H: heating; C: cooling)

Casted from solutions, the polymers containing fluorene units (**PF**, **PFR**, **PFRF**) formed thin depositions, whilst the semiflexible **PPEG** yielded a soft continuous film. Generally speaking, for optoelectronic applications, the thin films must be of good quality, continuous, without cracks or holes. This requirement is challenging for conjugated polyazomethines which are stiffed-rigid polymers with poor solubility, difficult to be processed from solution. In order to improve the quality of their films, the semicrystalline **PF**, **PFR** and **PFRF** were mixed with the semiflexible **PPEG** in three molar ratios: 50/50; 10/90; 1/99 to form homogeneous DMF solutions, and then casted on glass supports (Table 3). In this way, thin films were obtained and their features were investigated by POM. For the films obtained by using lower amounts of semicrystalline polymer (1%), rare birefringent spots dispersed in an amorphous phase could be seen (Figure 3d). Increase in the amount of semicrystalline polymer to 10% led to denser birefringent spots, some of them connected (Figure 3e). Further increase to 50 % resulted in

majority of spots being connected and forming birefringent hyphae-like network, reinforcing the film (Figure 3f). No crystallization of the **PPEG** was observed even after one month, indicating that mixing of polymers precluded its self-ordering process.

### 3.4 Photophysical properties

The photophysical properties of the polyazomethines were investigated by UV-vis absorption and photoluminescence spectroscopy in DMF solutions ( $10^{-5}$  M) and thin films.

In solution, all polymers presented at least two absorption bands (Figure 4). The polymers containing the bulky fluorene unit (**PFR**, **PFRF**) showed a third band in the shape as a shoulder at 310 nm. This additional band was attributed to the  $\pi$ - $\pi^*$  transitions in the fluorene unit linked to the main backbone by a  $sp^3$  – hybridized carbon atom, and thus electronically isolated.

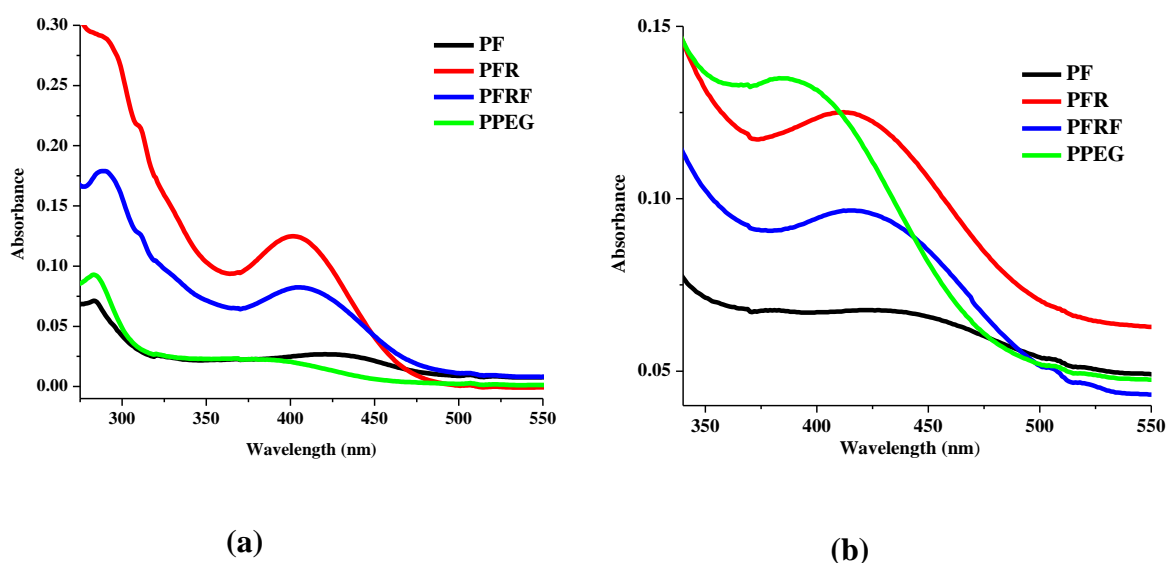


**Figure 4.** UV-vis spectra of the polyazomethines in a) DMF solutions and b) thin films

The first absorption band with the maximum around 285 nm originated from  $\pi$ - $\pi^*$  benzenoid transitions, as stated in literature [29, 36, 37].

The main absorption band ranging from 401 to 424 nm was assigned to the  $n$ - $\pi^*$  and  $\pi$ - $\pi^*$  transitions of the conjugated system *via* azomethine linkage [29, 37-40]. There is a good

correlation between the chemical structure of the polymers and the position of the absorption maximum of this band. Thus, (i) the absorption maximum was the mostly bathochromic shifted, at 424 nm for the polymer **PF** – reflecting the higher electronic delocalization along the phenothiazine-imine-fluorene conjugated chain. (ii) Disruption of the conjugation because of the tetrahedral carbon of the polymer **PFR** led to a lower wavelength of the absorption maximum, at 401 nm. (iii) The random distribution of the fluorene units, either into the polymer backbone or as bulky units (leading to shorter conjugated segments), shifted the absorption maximum to 405 nm, a value between the ones for **PF** and **PFR** polymers. The most hypsochromic shift of the band was recorded at 362 nm for the **PPEG** polymer, whose conjugated system was the shortest between a phenothiazine unit and two imine bonds. It is important to mention that the high dilution of the solution samples hindered the interaction between the polymers, thus the absorption behaviour was assigned to the isolated macromolecules. As phenothiazine is a strong electron donor chromophore (D) whilst azomethine and fluorene are electron acceptor moieties (A), the absorption band of highest wavelength was attributed to a D-A intramolecular charge transfer.

The optical band gap energy  $E_g$  was calculated using the Planck-Einstein relation for the maximum absorption wavelength [43]. As shown in Table 1, the  $E_g$  values are around 3 eV indicating an easy  $\pi$ -electron flowing along the polymer backbones, commonly met in the semiconducting organic polymers [42-45]. This reveals good electron delocalization from the donor to acceptor building blocks, aided by the withdrawing azomethine connection [29, 40-42]. All polymers showed similar absorption edge around 490 nm (2.5 eV). As expected, the **PF** polymer with the highest electron conjugation exhibited the lowest band gap.

Compared to the polyazomethine solutions, the corresponding thin films showed a bathochromic shift of the absorption maxima (Figure 4b) attributed to the re-distribution of the  $\pi$ -electrons in the conjugated backbones due to the  $\pi$ - $\pi$  interactions between D-A segments

found in a close proximity to each other in solid state [46]. The bathochromic shift was higher in the case of **PPEG** (21 nm), lower in the case of **PFR** and **PFRF** (10 and 11 nm, respectively) and totally missing in the case of **PF**, close related to the mobility of the macromolecules in solution and consequently to their tendency to self-organize. The band gap decreased correspondingly, reaching the value of the highest conjugated polymer **PF** (Table 1).

**Table 1.** UV-vis absorption parameters of the polyazomethines

Code	$\lambda_{\max, \text{sol.}}$	$E_g^*/\text{eV}_{\text{sol.}}$	$\lambda_{\max, \text{film}}$	$E_g^*/\text{eV}_{\text{film}}$
<b>PF</b>	283, 424	2.92	421	2.93
<b>PFR</b>	288, 310, 401	3.09	412	3.00
<b>PFRF</b>	290, 310, 405	3.06	415	2.98
<b>PPEG</b>	362	3.42	383	3.23

\* the energy gap spectroscopically determined from the absorption maxima ( $E_g = 1240/\lambda_{\max}$ )

The emission ability of the polymers was investigated by exciting with light corresponding to the maxima of the absorption wavelengths. In solution, all polymers emitted green light with an emission maximum from 506 to 548 nm, (Figure 5), regardless the wavelength of the exciting light.

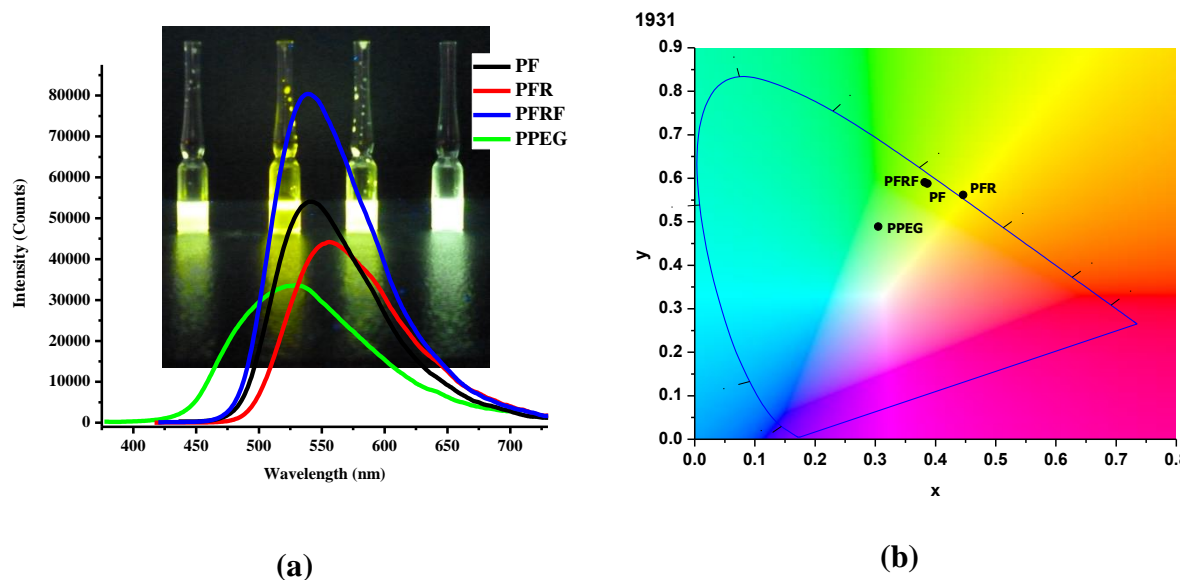


**Figure 5.** a) The emission spectra of the polyazomethine solutions excited at their absorption maximum of minimum energy and b) their chromaticity diagram (inset: polymer solutions illuminated with an UV lamp)



The absolute quantum yield, measured by using an integrating sphere, ranged from 28 to 56 % (Table 2) indicating efficient luminescence of the polyazomethines containing phenothiazine moiety. This is in contrast with the results obtained for the polyazomethines containing other chromophoric moieties such as homoaryl, thiophene, pyrrole, furan [46], quinolone [47], anthracene [48], pyridine [49] indicating that the phenothiazine donor unit is an excellent counterpart of the acceptor azomethine unit to promote luminescence properties. The high quantum yield of the poly(azomethine-phenothiazine) macromolecules appears to be a consequence of the good conjugation of the donor phenothiazine with the acceptor units, including azomethine bridge, increasing the rigidity which hinders the non-radiative decay of the excited state via dynamic intramolecular rotations [29, 50]. (The good conjugation of the phenothiazine donor with the azomethine acceptor forming a planar framework has already been proved on a model compound [29].) As can be seen in the chromaticity diagram, the emitted light is in the gamut of human vision: pure yellow-green light in the case of the polymers with more extended conjugation (**PF**, **PFR**, **PFRF**) and yellowish-green light of about 50% purity in the case of the semiflexible **PPEG** (Figure 4b).

It is important to note that the good quantum yields were registered by exciting the solution samples with the light corresponding to the absorption maximum of highest wavelength (lower energy). By exciting with light corresponding to the absorption maximum of lower wavelength (higher energy), lower quantum yield, around 4%, were obtained. This drastic diminishing in the emission efficiency suggests that the D-A segment with extended conjugation is the main fluorophore. Interesting enough, the high quantum yield of the random **PFRF** polymer appears to cumulate the individual values of the alternative **PF** and **PFR** polymers.

The values of the Stokes shifts, in solutions as well as films, were over 100 nm, resulting in an insignificant overlapping of the absorption and emission spectra. This means that the

photon loss by re-absorption phenomena is prevented, which is an important requirement for optoelectronic materials [29].

**Table 2.** Emission parameters of the polyazomethines in solution and film

Code	$\lambda_{em,sol}$	$\Phi^1_{sol}$	1931 CIE x; y <sup>2</sup> sol	$\lambda_{em,film}$	$\Phi^3_{film}$	1931 CIE x; y film	Stokes shift <sup>4</sup> sol/film
PF	541	39.62	0.31;0.49	544	13.2	0.27;0.49	117/123
PFR	548	29.44	0.37;0.59	532	9.6	0.31;0.52	147/120
PFRF	545	56.21	0.38;0.59	532	10.8	0.28;0.49	140/117
PPEG	506	28.39	0.45;0.55	529	8.14	0.29;0.49	144/146

<sup>1</sup>absolute fluorescence quantum yield in solution, at room temperature; <sup>2</sup>chromaticity coordinates; <sup>3</sup>absolute fluorescence quantum yield in film, at room temperature; <sup>4</sup>Stokes shift between the absorption and emission of the chromophores

As the real world applications requires solid state samples, the emission ability of the studied polyazomethines was also investigated on thin films, too. As it can be seen in table 2, they showed good quantum yield in solid state, their values ranging from 8 to 13 % (Table 2).

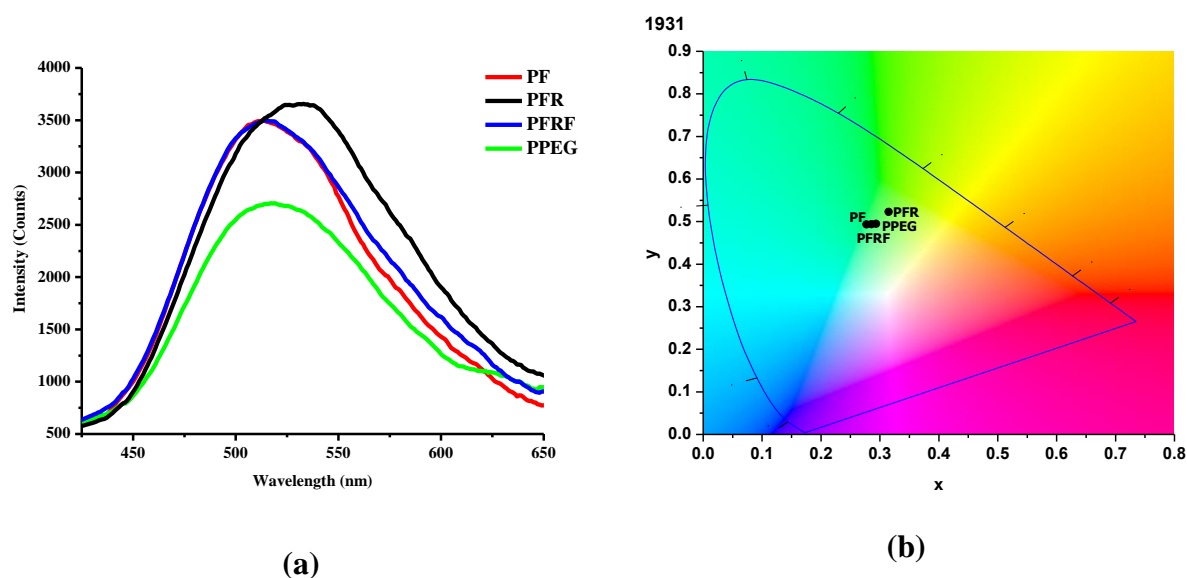


**Figure 6.** (a) The emission spectra of the polyazomethine films excited at their absorption maximum of minimum energy and (b) their chromaticity diagram

As a general rule, the good quantum yield in solution of the compounds with extended conjugation is weakened or quenched when in solid state because of the strong  $\pi$ - $\pi$  stacking interactions, which prompt the excimers formation, effect known as aggregation- caused quenching (ACQ) [51]. Moreover, as the extent of  $\pi$ -conjugation increases, the ACQ effect

becomes severer, as the aggregation tends to increase, too. In contrast, for the studied poly(azomethine-phenothiazine)s, a higher solid state quantum yield of 13% for the sample with the highest conjugation (**PF**) could be observed, compared to the other samples for which the quantum yield in thin films was around 10%. This could be explained by the structure of the phenothiazine fused ring. It was proved that phenothiazine adopts a butterfly shape, bended along the S N axis. This phenothiazine geometry promotes long intermolecular distances in solid state, which hinder the excimer and exciplex formation [29, 52]. This, cumulated with the higher extended conjugation in **PF**, led to a better quantum yield in solid state.

Furthermore, the emission of the of the poly(azomethine-phenothiazine)s was investigated on films obtained by dispersing the semicrystalline **PF**, **PFR**, **PFRF** into the semiflexible **PPEG** (Figure 7a). As can be seen in table 3, the emission intensity enhanced reaching a value of the quantum yield of 16 in the case of **3b** (PFRF-PPEG90/10). The colour of the emitted light shifted from yellow-greenish for pure polymer films (Figure 6b) to yellow-green domain, whilst the purity of the emitted light increased up to 80% (Figure 7b). This indicates that dispersing into the semiflexible matrix with similar chemical structure is beneficial to improving the film quality and photo physical properties.

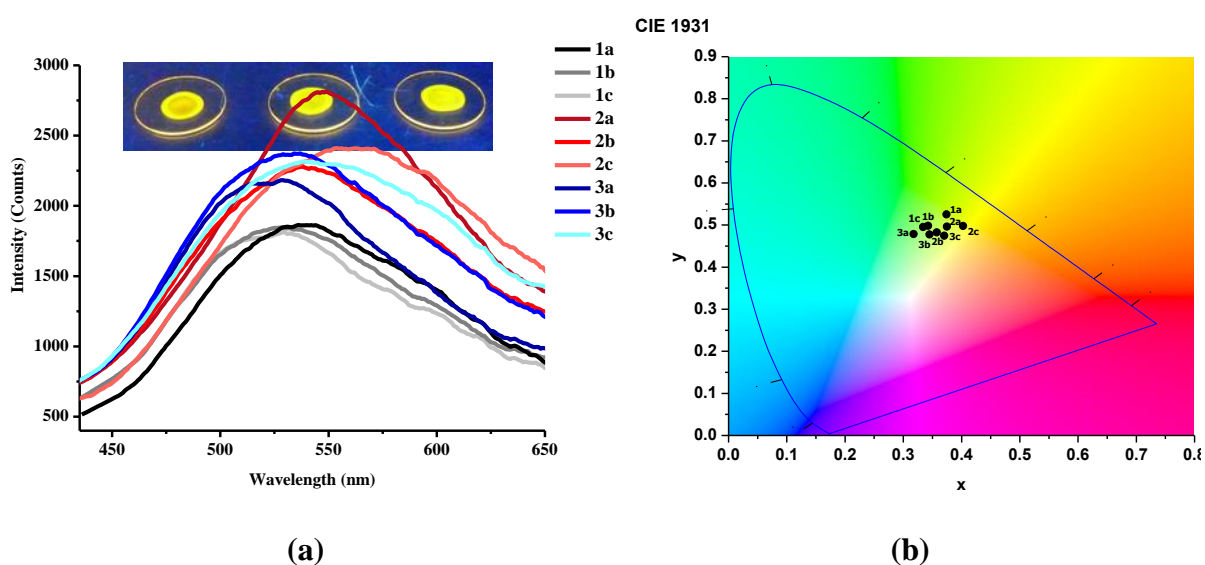


**Figure 7.** (a) The luminescence spectra and (b) chromaticity diagram of the poly(azomethine-phenothiazine)s mixtures (inset: films of 1a, 2a, 3a illuminated with an UV lamp)

**Table 3.** Luminescence parameters of the mixtures of **PPEG** with **PF**, **PFR** and **PFRF**

<b>Code</b>	<b>Molar ratio</b>	<b>1931 CIE x;y</b>	<b><math>\Phi</math></b>	<b>Color purity</b>
<b>1a</b>	PF-PPEG50/50	0.37/0.52	9.2	79
<b>2a</b>	PFR-PPEG50/50	0.37/0.49	12.1	70
<b>3a</b>	PFRF-PPEG50/50	0.31/0.47	12.1	41
<b>1b</b>	PF-PPEG10/90	0.34/0.49	13.4	61
<b>2b</b>	PFR-PPEG10/90	0.35/0.48	12.6	62
<b>3b</b>	PFRF-PPEG10/90	0.34/0.47	16	52
<b>1c</b>	PF-PPEG1/99	0.33/0.49	13.5	55
<b>2c</b>	PFR-PPEG1/99	0.40/0.49	11.5	75
<b>3c</b>	PFRF-PPEG1/99	0.37/0.47	14.9	53

## Conclusions

A series of poly(azomethine-phenothiazine)s was synthesized by polycondensation reaction of a phenothiazine dialdehyde with fluorene or PEG containing diamines, in mild reaction conditions, to give alternant or random polymers. The fluorene containing poly(azomethine-phenothiazine)s were semicrystalline with high melting points. The PEG containing polymer had low melting point due to its semiflexible nature. The connection of phenothiazine donor with fluorene acceptor *via* withdrawing azomethine bridge proved to be a valuable pathway for obtaining luminescent polymers with low band gap, large Stokes shift and good quantum yield in solid state. Mixing the semicrystalline polymers with the semiflexible one resulted in good quality films, with no cracks or holes, with luminescence efficiency reaching 16 %. The paper demonstrated that poly(azomethine-phenothiazine)s combine the advantage of being easy to synthesise and purify with the advantage of possessing high performance photophysical properties, with promising potential in organic optoelectronic applications.

**Funding:** This publication is part of a project funded by the European Union's **Horizon 2020 ERA research and innovation program under the grant agreement no: 667387** and Romanian National Authority for Scientific Research, MEN – UEFISCDI, project no. PN-II-PT-PCCA-2013-4-1861 (contract number 272/2014).

## References

- [1] A. Iwan, D. Sek, Processible polyazomethines and polyketanils: From aerospace to light-emitting diodes and other advanced applications, *Progr. Polym. Sci.* 33 (2008) 289–345.
- [2] W. Kleij, D. M. Tooke, A. L. Spek, J. N. H. Reek, A Convenient Synthetic Route for the Preparation of Nonsymmetric Metallosalphen Complexes, *Eur. J. Inorg. Chem.* 2005 (2005) 4626–4634.
- [3] M.F. Zaltariov, A. Vlad, M. Cazacu, M. Avadanei, N. Vornicu, M. Balan, S. Shova, Silicon-containing bis-azomethines: Synthesis, structural characterization, evaluation of the photo-physical properties and biological activity, *Spectrochim. Acta A.* 138 (2015) 38–48.
- [4] M. Holbach, X. Zheng, C. Burd, C. W. Jones, M. Weck, A Practical One-Pot Synthesis of Enantiopure Unsymmetrical Salen Ligands, *J. Org. Chem.* 71 (2006) 2903-2906.
- [5] İ. Kaya, S. Koyuncu, D. Şenol, Conductivity and band gap of oligo-2-[(4-fluorophenyl) imino methylene] phenol and some of its oligomer-metal complexes, *Eur. Polym. J.* 42 (2006) 3140–3144.
- [6] A. Zabulica, E. Perju, M. Bruma, L. Marin, Novel luminescent liquid crystalline polyazomethines. Synthesis and study of thermotropic and photoluminescent properties, *Liq. Cryst.* 41 (2014) 252–262.
- [7] N. Roy, B. Bruchmann, J.M. Lehn, Dynamers: dynamic polymers as self-healing materials, *Chem. Soc. Rev.* **44** (2015) 3786–3807.
- [8] A. Chao, I. Negulescu, D. Zhang, Dynamic Covalent Polymer Networks Based on Degenerative Imine Bond Exchange: Tuning the Malleability and Self-Healing Properties by Solvent, *Macromolecules* 49 (2016) 6277–6284.
- [9] P. Tyagi, A. Deratani, D. Bouyer, D. Cot, V. Gence, M. Barboiu, N.T. Phan, D. Bertin, Didier Gimes, Damien Quemener, Dynamic Interactive Membranes with Pressure-Driven Tunable Porosity and Self-Healing Ability, *Angew. Chem. Int. Edit.* 51 (2012) 7166–7170.
- [10] Z. Wei, J. Zhao, Y.M. Chen, P. Zhang, Q. Zhang, Self-healing polysaccharide-based hydrogels as injectable carriers for neural stem cells, *Scientific Reports* 6 (2016).

- [11] M. Iftime, S. Morariu, L. Marin, Salicyl-imine-chitosan hydrogels: Supramolecular architecturing as acrosslinking method toward multifunctional hydrogels, *Carbohydr. Polym.* 165 (2017) 39–50.
- [12] Marin, L.; Morariu, S.; Popescu, M. C.; Nicolescu, A.; Zgardan, C.; Simionescu B. C.; Barboiu, M. Out-of-Water Constitutional Self-Organization of Chitosan–Cinnamaldehyde Dynagels. *Chem. Eur. J.* 20 (2014) 4814–4821.
- [13] M. Barboiu, Artificial water channels, *Angew. Chem. Int. Edit.* 51 (2012) 11674–11676.
- [14] L. Marin, D. Ailincăi, M. Calin, D. Stan, C.A. Constantinescu, L. Ursu, F. Doroftei, M. Pinteala, B.C. Simionescu, M. Barboiu, Dynameric Frameworks for DNA Transfection, *ACS Biomat. Sci. Eng.* 2 (2016) 104–111.
- [15] D. Navarathne, W.G. Skene, Towards Electrochromic Devices Having Visible Color Switching Using Electronic Push-Push and Push-Pull Cinnamaldehyde Derivatives, *ACS Appl. Mater. Inter.* 5 (2013) 12646–12653.
- [16] A. Iwan, P. Bilski, M. Klosowski, Thermoluminescence measurements of liquid crystal azomethines and poly(azomethine)s with different shapes as thermo-detectors, *J. Lumin.* 130 (2010) 2362–2367.
- [17] Avci, I. Kaya, A new selective fluorescent sensor for Zn(II) ions based on poly(azomethine-urethane), *Tetrahedron Lett.* 56 (2015) 1820–1824.
- [18] S.M. Kim, J.S. Kim, D.M. Shin, Y.K. Kim, Y. Ha, Synthesis and application of the novel azomethine metal complexes for the organic electroluminescent devices, *Bull. Korean Chem. Soc.* 22 (2001) 743–747.
- [19] M. E. Nowak, J. Sanetra, M. Grucela, E. Schab-Balcerzak, Azomethine naphthalene diimides as component of active layers in bulk heterojunction solar cells, *Materials Letters* 157 (2015) 93–98.
- [20] B. Vercelli, M. Pasini, A. Berlin, J. Casado, J.T. Lopez Navarrete, R.P. Ortiz, G. Zotti, Phenyl- and Thienyl-Ended Symmetric Azomethines and Azines as Model Compounds for n-Channel Organic Field Effect Transistors: An Electrochemical and Computational Study, *J. Phys. Chem. C* 118 (2014) 3984–39933.
- [21] M. Koole, R. Frisenda, M.L. Petrus, M.L. Perrin, H.S.J. van der Zant, T.J. Dingemans, Charge transport through conjugated azomethine-based single molecules for optoelectronic applications, *Org. Electron.* 34 (2016) 38–41.
- [22] B. Ma, H. Zhang, Y. Wang, Y.X. Peng, W. Huang, M.K. Wang, Y. Shen, Visualized acid-base discoloration and optoelectronic investigations of azines and azomethines having

- double 4-[N,N-di(4-methoxyphenyl)amino]phenyl terminals, *J. Mat. Chem. C* 3 (2015) 7748–7755.
- [23] D. Isik, C. Santato, S. Barik, W.G. Skene, Charge-Carrier Transport in Thin Films of p-Conjugated Thiopheno-Azomethines, *Org. Electron.* 13 (2012) 3022–3031.
- [24] Y. Park, J.H. Lee, D.H. Jung, S.H. Liu, Y.H. Lin, L.Y. Chen, C.C. Wud, J. Park, An aromatic imine group enhances the EL efficiency and carrier transport properties of highly efficient blue emitter for OLEDs, *J. Mater. Chem.* 20 (2010) 5930–5936.
- [25] D. Sek, A. Iwan, B. Jarzabek, B. Kaczmarczyk, J. Kasperczyk, Z. Mazurak, M. Domanski, K. Karon, M. Lapkowski, Hole transport triphenylamine- azomethine conjugated system: Synthesis and optical, photoluminescence, and electrochemical properties, *Macromolecules* 41 (2008) 6653–6663
- [26] L. Marin, D. Timpu, V. Cozan, G.I. Rusu, A. Airinei, Solid State Properties of Thin Films of New Copoly(azomethine-sulfone)s, *J. Appl. Polym. Sci.* 120 (2011) 1720–1728.
- [27] L. Marin, A. van der Lee, S. Shova, A. Arvinte, M. Barboiu, Molecular amorphous glasses toward large azomethine crystals with aggregation-induced emission, *New J. Chem.* 39 (2015) 6404–6420.
- [28] M. Grucela-Zajac, K. Bijak, S. Kula, M. Filapek, M. Wiacek, H. Jameczek, L. Skorka, J. Gasiorowski, K. Hingerl, N. S. Sariciftici, N. Nosidlak, G. Lewinska, J. Sanetra, E. Schab-Balcerzak, (photo)physical properties of new molecular glasses end-capped with thiophene rings composed of diimide and imine units, *J. Phys. Chem. C* 118 (2014) 13070–13086.
- [29] A. Zabulica, M. Balan, D. Belei, M. Sava, B. C. Simionescu, L. Marin, Novel luminescent phenothiazine-based Schiff bases with tuned morphology. Synthesis, structure, photophysical and thermotropic characterization, *Dyes Pigments* 96 (2013) 686–698.
- [30] A. Danilevicius, J. Ostrauskaite, J.V. Grazulevicius, V. Gaidelis, V. Jankauskas, Z. Tokarski, N. Jubran, J. Sidaravicius, S. Grevys, A. Dzena, Photoconductive glass-forming phenothiazine-based hydrazones, *J. Photochem. Photobio. A* 163 (2004) 523–528.
- [31] E. Tozzo, S. Romera, M. P. dos Santos, M. Muraro, R. H. de A. Santos, L.M. Liaoc, L. Vizotto, E. R. Dockal, Synthesis, spectral studies and X-ray crystal structure of N,N0-(±)-trans-1,2-cyclohexylenebis(3-ethoxysalicylideneamine) H<sub>2</sub>(t-3-EtOsalcxn), *J. Mol. Struct.* 876 (2008) 110–120.
- [32] K.C. Gupta, A. K. Sutar, Catalytic activities of Schiff base transition metal complexes, *Coordin. Chem. Rev.* 252 (2008) 1420–1450.

- [33] A. Carreño, M. Gacitúa, D. Páez-Hernández, R. Polanco, M. Preite, J. A. Fuentes, G. C. Mora, I. Chávez, R. Arratia-Pérez, Spectral, theoretical characterization and antifungal properties of two phenol derivatives Schiff base with an intramolecular hydrogen bond, *New J. Chem.*, **39** (2015), 7822–7831.
- [34] L. Marin, D. Ailincăi, M. Mares, E. Paslaru, M. Cristea, V. Nica, B.C. Simionescu, Imino-Chitosan Biopolymeric Films. Obtaining, Self-assembling, Surface and Antimicrobial Properties, *Carbohydr. Polym.* 117 (2015) 762–770.
- [35] J. Meng, X. Tang, W. Li, H. Shi, X.X. Zhang, Crystal structure and thermal property of polyethylene glycol octadecyl ether, *Thermochim. Acta* 558 (2013) 83–86.
- [36] İ. Kaya, M. Yıldırım, M. Kamacı, Synthesis and characterization of new polyphenols derived from *o*-dianisidine: The effect of substituent on solubility, thermal stability, and electrical conductivity, optical and electrochemical properties, *Eur. Polym. J.* 45 (2009) 1586–1598.
- [37] W.L. Lim, C.W. Oo, Y.S.L. Choo, S.T. Looi, New generation of photosensitive poly(azomethine)esters: Thermal behaviours, photocrosslinking and photoluminescence studies, *Polymer* 71 (2015) 15–22.
- [38] S. Dineshkumar, A. Muthusamy, P. Chitra, S. Anand, Synthesis, characterization, optical and electrical properties of thermally stable polyazomethines derived from 4,4'-oxydianiline, *J. Adhes. Sci. Technol.* 29 (2015) 2605–2621.
- [39] I. Cianga, M. Ivanoiu, Synthesis of poly(Schiff-base)s by organometallic processes, *Eur. Polym. J.* 42 (2006) 1922–1933.
- [40] L. Marin, E. Perju, D. Damaceanu, Designing thermotropic liquid crystalline polyazomethines based on fluorene and / or oxadiazole chromophores, *Eur. Polym. J.* 47 (2011) 1284–1299.
- [41] M.D. Damaceanu, C.P. Constantin, L. Marin, Insights into the effect of donor-acceptor strength modulation on physical properties of phenoxazine-based imine dyes, *Dyes Pigments* 134 (2016) 382–396.
- [42] E. Gal, L. Găină, C. Cristea, V. Munteanu, L. Silaghi-Dumitrescu, The influence of bonding topology on the electronic properties of new Schiff bases containing phenothiazine building blocks, *J. Electroanal. Chem.* 770 (2015) 14–22.
- [43] L. Marin, V. Harabagiu, A. van der Lee, A. Arvinte, M. Barboiu, Structure-directed functional properties of symmetrical and unsymmetrical Br-substituted Schiff-bases, *J. Molec. Struct.*, 1049 (2013), 377–385.



- [44] C.I. Simionescu, M. Grigoras, I. Cianga, N. Olaru, Synthesis of new conjugated polymers with Schiff base structure containing pyrrolyl and naphthalene moieties and HMO study of the monomers reactivity, *Eur. Polym. J.* 34 (1998) 891–898.
- [45] D. Seo, J. Park, T.J. Shin, P.J. Yoo, J. Park, K. Kwak, Bathochromic shift in absorption spectra of conjugated polymer nanoparticles with displacement along backbones, *Macromol. Res.* 23 (2015) 574–577.
- [46] S. Dufresne, W.G. Skene, Optoelectronic property tailoring of conjugated heterocyclic azomethines – the effect of pyrrole, thiophene and furans, *J. Phys. Org. Chem.* 25 (2012) 211–221.
- [47] S. Kotowicz, M. Siwy, M. Filapek, J.G. Malecki, K. Smolarek, J. Grzelak, S. Mackowski, A. Slodek, E. Schab-Balcerzak, New donor-acceptor-donor molecules based on quino-line acceptor unit with Schiff base bridge: synthesis and characterization, *J. Lumin.* 183 (2017) 458–469.
- [48] E. Schab-Balcerzak, M. Grucela, G. Malecki, S. Kotowicz, M. Siwy, H. Janeczek, S. Golba, A. Praski, Azomethine diimides end-capped with anthracene moieties: Experimental and theoretical investigations, *J. Mol. Struct.* 1128 (2017) 462–470.
- [49] A. Carreno, M. Gacitua, J.A. Fuentes, D. Paez-Hernandez, C. Araneda, I. Chavez, M. Soto-Arriaza, J.M. Manriquez, R. Polanco, G.C. Mora, C. Otero, W.B. Swords, R. Arrati-Perez, Theoretical and experimental characterization of a novel pyridine benzimidazole: suitability for fluorescence staining in cells and antimicrobial properties, *New J. Chem.* 40 (2016) 2362–2375.
- [50] L. Magginia, D. Bonifazi, Hierarchised luminescent organic architectures: design, synthesis, self-assembly, self-organisation and functions, *Chem. Soc. Rev.* 41 (2012) 211–241.
- [51] J. B. Birks, *Photophysics of Aromatic Molecules*, Wiley, London, 1970.
- [52] A. Bejan, S. Shova, M.D. Damaceanu, B.C. Simionescu, L. Marin, Structure-Directed Functional Properties of Phenothiazine Brominated Dyes: Morphology and Photophysical and Electrochemical Properties, *Crystal Growth Des.* 16 (2016) 3716–3730.